

Testing coupled dark energy with next-generation large-scale observations

Luca Amendola¹, Valeria Pettorino², Claudia Quercellini³, Adrian Vollmer¹

¹ *Institut fuer Theoretische Physik, Universitaet Heidelberg,
Philosophenweg 16, D-69120 Heidelberg, Germany.*

² *SISSA, Via Bonomea 265, 34136 Trieste, Italy,*

³ *University of Rome Tor Vergata, Via della Ricerca Scientifica, 1 - I-00133 Roma (Italy)*

(Dated: May 28, 2018)

Coupling dark energy to dark matter provides one of the simplest way to effectively modify gravity at large scales without strong constraints from local (i.e. solar system) observations. Models of coupled dark energy have been studied several times in the past and are already significantly constrained by cosmic microwave background experiments. In this paper we estimate the constraints that future large-scale observations will be able to put on the coupling and in general on all the parameters of the model. We combine cosmic microwave background, tomographic weak lensing, redshift distortions and power spectrum probes. We show that next-generation observations can improve the current constraint on the coupling to dark matter by two orders of magnitude; this constraint is complementary to the current solar-system bounds on a coupling to baryons.

I. INTRODUCTION

Several observational campaigns will be launched in the next few years to advance our knowledge of the matter distribution from redshifts of order $z \leq 0.5$ (the depth of the SDSS [1] and 2dF [2] surveys) to $z \leq 2 - 3$ (the range of satellite missions like Euclid [3] and of ground-based surveys like LSST [4], DES [5], etc). These surveys will map hundreds of millions of galaxy redshifts and billions of galaxy images distributed across almost the full accessible sky. The information contained in these data will occupy the cosmologists for years to come and it is very useful already at this stage to foresee what these data can tell us about the currently investigated cosmological models. Several works have been devoted to forecasting future constraints with future wide surveys and a small selection of the recent ones can be found in Ref. [6–10].

The main science drivers for most of these large-scale enterprises is the quest for dark energy (DE). Even if we get very accurate knowledge of the cosmic background expansion and therefore of the dark energy equation of state, this will not be enough to distinguish among competing models. In fact, in the models in which dark energy clusters or gravity is modified (see e.g. [11]), the linear growth of clustering is in general not completely fixed by background observables. Mapping the linear clustering has been identified as the main probe of modification of gravity or, more in general, of non-standard dark energy models.

The main probes of matter clustering are the weak lensing and the galaxy power spectrum $P(k)$ and indeed most large scale surveys aim at mapping one or both of these quantities. For instance Euclid, probably the most ambitious project to date, sets as goal the mapping of half the sky both in imaging and in broad-band spectroscopy, with an average redshift of order unity and a maximal useful redshift around 2 or 3. Combining weak lensing and $P(k)$ gives the opportunity to break several degeneracies among the cosmological parameters and to directly measure the growth function.

Both WL and $P(k)$ probe the universe at relatively small redshifts. A much longer lever arm is obtained by combining them with the cosmic microwave background, in particular employing the specifics of the Planck mission. In this way we can tighten sensibly the constraints on all the cosmological parameters.

In this paper we focus on one particular class of dark energy models that includes typical features of modified gravity models, the coupled dark energy model ([12–14], see e.g. [11] for a review). The idea behind this model is very simple: when dark energy is promoted to a scalar field ϕ , as in the vast majority of DE models and also as in the prototypical accelerated expansion, inflation, one naturally wonders whether this field could be mediating a force among matter particles. This is indeed the same phenomenology as in the Brans-Dicke model, except that now we require this field also to drive acceleration and therefore to be dominant and to carry a potential. In this paper we model the ϕ potential as an inverse power-law $V \sim \phi^{-\alpha}$, as in the Ratra-Peebles scenario [15]. This one-parametric family is simple but gives us enough freedom to explore the dependence of the results on the potential slope and therefore on the equation of state. The phenomenology of this interaction can be immediately grasped by writing down the energy-momentum conservation equations:

$$T_{(m)\nu;\mu}^{\mu} = \beta T_{(m)}\phi_{;\nu} \quad (1)$$

$$T_{(\phi)\nu;\mu}^{\mu} = -\beta T_{(m)}\phi_{;\nu} \quad (2)$$

where the subscripts m, ϕ denote matter and dark energy, respectively and where β is the coupling constant. While β could also be a coupling function $\beta(\phi)$ (see e.g. [16–18]), in this paper we restrict ourselves for simplicity to a constant value. A coupled particle of mass m will respond to this interaction by following in the Newtonian regime the scalar-gravitational potential

$$U = -\frac{Gm}{r}(1 + 2\beta^2 e^{-m_\phi r}) \quad (3)$$

where m_ϕ depends on the field potential. For a dark energy field one expects the interaction scale $1/m_\phi$ to be of astrophysical size. The parameter β^2 quantifies therefore the deviation from Newtonian dynamics. Any indication that $\beta \neq 0$ would of course show a fundamental modification of nature’s law. The main goal of this paper is to forecast the future constraints on β and to see how all the other cosmological parameters depend on it.

Since gravity now is supplemented by an additional scalar mediator, the resulting scalar-tensor force deviates from Einstein’s (and from Newton’s) one and this gives rise to a number of observable differences with respect to the uncoupled models, both at the background and at the perturbation level. The expansion is generally modified when β is non-zero. In particular, it has been shown in [19] that for most potentials DE is not negligible in the past, contrary to the cosmological constant case and to models that do not drastically deviate from it. Adopting the Ratra-Peebles potential one finds that the evolution of the scalar field during the matter domination is controlled by the coupling β and the density fraction Ω_ϕ is proportional to β^2 . As a consequence, the expansion rate H , given in terms of the effective equation of state w_{eff} by

$$\frac{H'}{H} = -\frac{3}{2}(1 + w_{\text{eff}}) \quad (4)$$

is modified. We define here $w_{\text{eff}} \equiv p_t/\rho_t$, where p_t and ρ_t are the total pressure and energy density contributions respectively. The value of w_{eff} decreases from $1/3$ in radiation dominated era to

$$w_{\text{eff}} \approx \frac{2}{3}\beta^2 \quad (5)$$

during matter dominated epoch, where the dominant contribution to p_t is given by the scalar field. More recently, dark energy dominates and w_{DE} tends to -1 : the higher the coupling, the fastest is the transition between matter and dark energy dominated era. This behavior is illustrated in Fig.(1) Accordingly, properties as the age of the Universe and the distance to last scattering (and therefore the position of the acoustic peaks) do also depend on β and this allows to put stronger constraints on it. In fact the best constraints on β so far come from the CMB data of WMAP, $|\beta| \leq 0.15$ [20, 21]. We stress that here we consider massless neutrinos but it is important to notice that if neutrinos are massive higher values of the coupling ($\beta \leq 0.2$) can be allowed [22]. At the perturbation level, the extra pull induced by the scalar force adds to gravity and speeds up the perturbation growth, resulting in further possible constraints.

Any modification of gravity has to pass the strong bounds from local experiments, both in laboratory and in the solar system or other astrophysical sources (see e.g. [23–25]). This can be achieved in several ways by the so-called chameleon [26, 27] or Vainshtein mechanisms [28] but here we adopt a simpler way out: we assume that baryons are uncoupled. In this case, all local experiments are bypassed and cosmology becomes the only way to observe the coupling.

II. COUPLED DARK ENERGY

We consider coupled dark energy cosmologies as described by the lagrangian:

$$\mathcal{L} = -\frac{1}{2}\partial^\mu\phi\partial_\mu\phi - U(\phi) - m(\phi)\bar{\psi}\psi + \mathcal{L}_{\text{kin}}[\psi], \quad (6)$$

in which the mass of matter fields ψ coupled to the DE is a function of the scalar field ϕ . In the following we will consider the case in which DE is only coupled to cold dark matter (CDM, hereafter denoted with a subscript c). The choice $m(\phi)$ specifies the coupling and as a consequence the source term $Q_{(\phi)\mu}$ via the expression:

$$Q_{(\phi)\mu} = \frac{\partial \ln m(\phi)}{\partial \phi} \rho_c \partial_\mu \phi. \quad (7)$$

Due to the constraint of conservation of the total energy-momentum tensor, if no other species is involved in the coupling, $Q_{(c)\mu} = -Q_{(\phi)\mu}$.

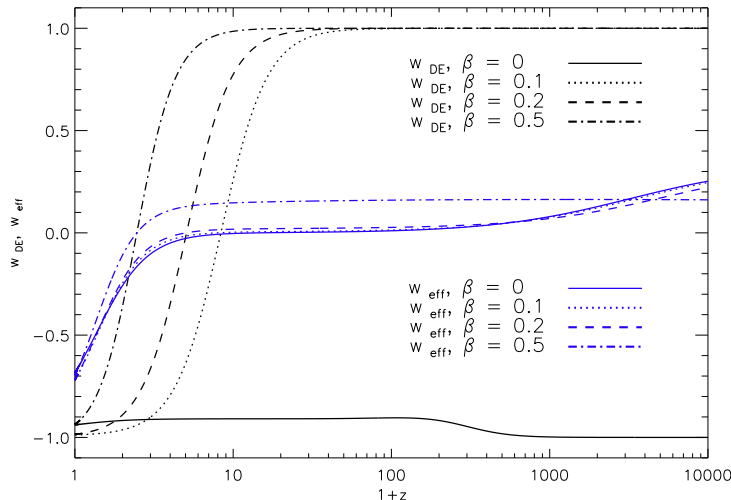


Figure 1: Evolution of w_{eff} for various values of β .

The conservation equations for the energy densities of each coupled species are:

$$\begin{aligned}\rho'_\phi &= -3\mathcal{H}\rho_\phi(1+w_\phi) - Q_{(\phi)0} \quad , \\ \rho'_c &= -3\mathcal{H}\rho_c + Q_{(\phi)0}\end{aligned}\quad (8)$$

(where primes denote differentiation with respect to conformal time and $\mathcal{H} = aH$ is the conformal Hubble function) plus the standard conservation equation for baryons. Here we have treated each component as a fluid with $T^\nu_{(\alpha)\mu} = (\rho_\alpha + p_\alpha)u_\mu u^\nu + p_\alpha\delta^\nu_\mu$, where $u_\mu = (-a, 0, 0, 0)$ is the fluid 4-velocity and $w_\alpha \equiv p_\alpha/\rho_\alpha$ is the equation of state. The class of models considered here corresponds to the choice:

$$m(\phi) = m_0 e^{-\beta \frac{\phi}{M}} \quad , \quad (9)$$

with the coupling term equal to

$$Q_{(\phi)0} = -\frac{\beta}{M}\rho_c\phi' \quad . \quad (10)$$

Equivalently, the scalar field evolves according to the Klein-Gordon equation:

$$\phi'' + 2\mathcal{H}\phi' + a^2 \frac{dV}{d\phi} = a^2\beta\rho_c \quad . \quad (11)$$

Throughout this paper we choose an inverse power law potential defined as:

$$V = V_0\phi^{-\alpha} \quad (12)$$

with α and V_0 constants. When the coupling is absent, this potential leads to a well-known transient tracking solution [12, 13, 29] in which

$$w_{DE} \approx -\frac{2}{\alpha+2} \quad (13)$$

which sets up just before the final dark energy domination; after this regime, asymptotically $w_{DE} \rightarrow -1$. When $\beta \neq 0$ but small, this tracking regime is also approximately true but squeezed between the modified matter era with $w_{\text{eff}} \approx 2\beta^2/3$ and the final phase with $w_{DE} \rightarrow -1$ and therefore barely visible. Current supernovae Ia constraints impose an upper limit $\alpha \leq 0.2$.

Various choices of couplings have been investigated in literature [12–14, 30–36]. Analysis of the models and constraint on these couplings have been obtained in several ways, including spherical collapse ([37, 38] and references therein), time renormalization group [39], N -body simulations [17, 40, 41] and effects on supernovae, CMB and cross-correlation of CMB and LSS [7, 9, 19–22, 42–44]. Refs. [7, 9] are particularly similar in spirit to our work. However

there are several differences. First, the coupling is different since we use the coupling induced by a scalar-tensor model. Second, we include the galaxy clustering probe (baryon acoustic oscillations or BAO, redshift distortions and full $P(k)$ shape). Third, we include the potential slope α as an additional parameter. Fourth, we use the updated Euclid Definition phase [3] specification (there is some change with respect to the ones in the Assessment phase defined in the yellow book [45]; in particular, the total area has been reduced from 20,000 to 15,000 square degrees).

III. METHODOLOGY

In this section we present the methodology we used to derive predictions on cosmological parameter constraining power from a combination of upcoming and future datasets, namely galaxy power spectrum sliced in several redshift bins, CMB angular power spectra (temperature and polarization) and Weak Lensing power spectrum. The statistical method chosen to do forecasts is the Fisher Matrix analysis. In order to derive the contour confidence regions in the parameter space both the likelihood of the data and the distribution of parameter values is assumed to be Gaussian.

Suppose to have an observable $\mathbf{X}_{\text{obs}} = [X_1, \dots, X_N]$ which is a function of the parameter set $\Theta = [\theta_1, \dots, \theta_n]$. Then the probability of estimating unknown parameters based on known outcomes is

$$\mathcal{L}(\mathbf{X}_{\text{obs}}/\theta) \propto \exp(\mathbf{X}_{\text{obs}} - \mathbf{X}(\theta))^T \mathcal{C}^{-1}(\mathbf{X}_{\text{obs}} - \mathbf{X}(\theta)) \quad (14)$$

where $\mathbf{X}(\theta)$ is the theoretical prediction for \mathbf{X}_{obs} as a function of θ and \mathcal{C} is the covariance matrix of the observed components. By assuming priors on each parameter, one is in principle able to sample this function at reasonable accuracy level.

In the Fisher Matrix formalism the observed outcome is the mean values of the observables \mathbf{X}_μ assumed as the null hypothesis. This method allows a quick way to estimate errors on cosmological parameters, given errors in observable quantities. The Fisher matrix is defined as the Hessian of the log-likelihood function \mathcal{L} ,

$$F_{ij} = \left\langle -\frac{\partial^2 \log \mathcal{L}(\mathbf{X}_\mu/\theta)}{\partial \theta_i \partial \theta_j} \right\rangle \quad (15)$$

such that if the parameters are assumed to be gaussianly distributed their likelihood can be written as

$$\mathcal{L}(\theta) \propto \exp -\frac{1}{2} \sum_{ij} \theta_i F_{ij} \theta_j. \quad (16)$$

By the Cramer-Rao inequality, a model parameter θ_i cannot be measured to a precision better than $(F_{ii})^{-1/2}$ when all other parameters are fixed, or a precision $((F^{-1})_{ii})^{1/2}$ when all other parameters are marginalized over. In practice, the Fisher matrix is a good approximation to the uncertainties as long as the likelihood can be approximated by a Gaussian, which is generally the case near the peak of the likelihood and therefore in cases when the parameters are measured with small errors. Conversely, if the errors are large, then the likelihood is typically non-Gaussian, and the constraint region is no longer elliptical but characteristically banana-shaped. In this case, the Fisher matrix typically underestimates the true parameter errors and degeneracies, and one should employ the full likelihood calculation approach to error estimation.

In this work the observables \mathbf{X} correspond to the galaxy power spectrum measured by a future experiment like Euclid, the imminent Planck CMB angular power spectra (TT, EE, BB and TE components) and the weak lensing power spectrum as detected by a future Euclid-like mission. The cosmological parameter set θ comprises the dimensionless Hubble parameter h , the dark matter and baryon density parameters Ω_c and Ω_b , respectively, the spectral index of primordial perturbations n_s , the coupling constant β and the slope of the dark energy potential α . We assume a flat geometry. In the Fisher formalism, all the information about the experiment is embedded in the covariance matrix: hence we need to define the suitable covariance for each observable/experiment.

As a fiducial model we assume the values of parameters shown in Tab.I. Other fiducial parameters needed for the various probes are specified later on. Since the main cosmological effects depend on β^2 (for small β) we use β^2 , rather than β , as parameter. This confines the parameter volume to $\beta^2 \geq 0$. Choosing the fiducial at $\beta^2 = 0$, in the Fisher approximation the cut $\beta^2 \geq 0$ does not alter the confidence regions. Also, we choose $\alpha = 0.2$ as fiducial, but this should not have an important impact since the tracking regime lasts very shortly; we tested also the case $\alpha = 0.1$. The other fiducial values are taken from WMAP7 [46] although since $\alpha \neq 0$ our fiducial model is not exactly Λ CDM.

All the derivatives of the Fisher matrix are performed numerically by evaluating the spectra at two values $\theta_i(1 \pm \varepsilon)$ where θ_i is a cosmological parameter (for parameters whose fiducial is zero we use $\theta_i \pm \varepsilon$). Here we chose $\varepsilon = 0.03$ but we also tested that for $\varepsilon = 0.06$ the final constraints change by at most 20%.

Parameter	Value
$\Omega_c h^2$	0.1116
H_0	70.3 km s ⁻¹ Mpc ⁻¹
$\Omega_b h^2$	0.02227
n_s	0.966
β^2	0
α	0.2
A	2.42×10^{-9}

Table I: Cosmological fiducial model: parameters are consistent with the WMAP 7 year results for a Λ CDM cosmology [46, 47] plus a coupling.

Planck	Channel [GHz]	FWHM	σ_T [$\mu K/K$]
$f_{\text{sky}} = 0.85$	70	14'	4.7
	100	10'	2.5
	143	7.1'	2.2

Table II: Planck experimental specifications [48]. FWHM is the Full Width at Half Maximum of the beam, assuming a Gaussian profile and expressed in arc-minutes. The polarization sensitivity is $\sigma_P = \sqrt{2}\sigma_T$.

IV. RESULTS FROM CMB DATA

The coupling has two main effects on the CMB: 1) it moves the position of the acoustic peaks to larger ℓ 's due to the increase in the last scattering surface distance (sometimes called projection effect, [14] and references therein); 2) it reduces the ratio of baryons to dark matter at decoupling with respect to its present value, since coupled dark matter dilute faster than in an uncoupled model. Both effects are clearly visible in Fig. (2) for some values of β .

We use the Fisher Matrix method described in section III to predict confidence contours for the cosmological parameter set $\Theta \equiv \{\beta^2, \alpha, \Omega_c, h, \Omega_b, n_s, \log A\}$, where A is the spectrum normalization, around the chosen fiducial model. The fiducial value of A is chosen to be $A = 2.42 \times 10^{-9}$, as in WMAP7 best fit for Λ CDM [46, 47]. For our CMB analysis, we use Planck satellite [48] specifications and include three frequency channels, each characterized by the experimental specifications illustrated in Tab.II. For each channel we specify the FWHM (Full Width at Half Maximum) of the beam when assuming a Gaussian profile and the temperature sensitivity σ_T . The polarization sensitivity is given by $\sigma_P = \sqrt{2}\sigma_T$. To each theoretical C_l spectrum, we add a noise spectrum given by:

$$N_l = (\theta\sigma)^2 \exp(l(l+1)/l_b^2) \quad (17)$$

where l_b is given by $l_b \equiv \sqrt{8 \ln 2}/\theta$ and θ is the FWHM.

We obtained the CMB spectra by modifying the CAMB code [49] including the coupling; the output have been compared to an independent code [20] that is build on CMBFAST and the agreement was better than 1%. The initial conditions needed to obtain the desired present values of the cosmological parameters must be found by trial and error, through an iterative routine.

The main results are in Fig.(3), obtained marginalizing over all parameters except those in the axes. Notice the sharp degeneracy β^2 vs. h , in agreement with [20], and with Ω_c and n_s . This can be understood in the context of coupled dark energy. With respect to a cosmological constant model, coupled dark matter dilutes more rapidly so that ρ_m was higher in the past, leading to a faster expansion and a consequent smaller size of the sound horizon at the last scattering surface, not fully compensated by the faster expansion after decoupling; this moves the acoustic peak towards larger ℓ s, an effect which is degenerated with an increase of h (Fig.(3), central panel). On the other hand, a stronger coupling decreases the peak amplitudes because ρ_b/ρ_m at decoupling gets smaller: this effect is compensated by lower values of Ω_c or by higher values of the spectral index n_s . In Table (IV) we report the fully marginalized 1σ errors for all parameters; for convenience of comparison we also report here the results of the next sections.

In Fig. (4) instead we fix h , i.e. we assume that its fiducial value has a negligible error. If we fix h and n_s we get Fig. (5); the other contours do not improve with respect to fixing h only (see Table IV). The significant improvement on the errors shows that there is much to gain by reducing the errors on h, n_s . The error on β^2 goes from 0.009 (fully marginalized) to 0.004 (fixing both h and n_s), with a consequent better estimation of Ω_c .

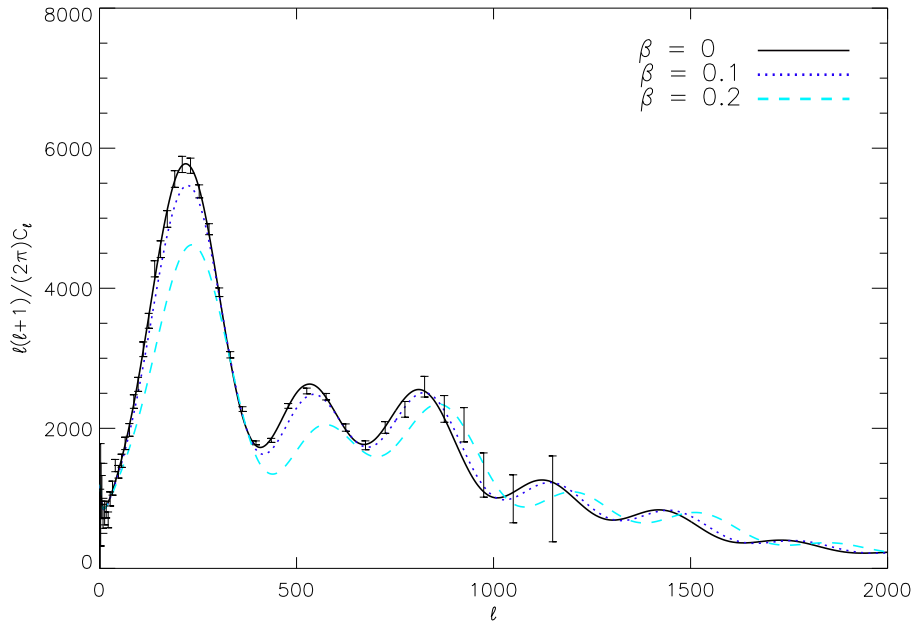


Figure 2: CMB unlensed TT temperature spectra for three values of β . Data are taken from WMAP7 [46].

Parameter	σ_i CMB	σ_i $P(k)$	σ_i WL
β^2	0.0094	0.0015	0.012
α	0.55	0.12	0.083
Ω_c	0.022	0.010	0.012
h	0.15	0.036	0.039
Ω_b	0.00087	0.0022	0.010
n_s	0.014	0.034	0.026
σ_8	-	0.0084	0.024
$\log A$	0.0077	-	-

Table III: $1-\sigma$ errors for the set $\Theta \equiv \{\beta^2, \alpha, \Omega_c, h, \Omega_b, n_s, \sigma_8, \log A\}$ of cosmological parameters, using CMB data, $P(k)$ and Weak Lensing (WL). Here and in all the following tables the errors are fully marginalized.

Parameter	σ_i CMB	σ_i CMB(\bar{h})	σ_i CMB(\bar{h}, \bar{n}_s)
β^2	0.0094	0.0044	0.0041
α	0.55	0.52	0.44
Ω_c	0.022	0.011	0.0079
h	0.15	-	-
Ω_b	0.00087	0.00081	0.00043
n_s	0.014	0.012	-
σ_8	0	0	0
$\log(A)$	0.0077	0.0074	0.0057

Table IV: $1-\sigma$ errors using CMB for the set $\Theta \equiv \{\beta^2, \alpha, \Omega_c, h, \Omega_b, n_s, \sigma_8, \log(A)\}$ (left column), $\Theta \equiv \{\beta^2, \alpha, \Omega_c, \Omega_b, n_s, \sigma_8, \log(A)\}$ (middle column, h fixed to the reference value), $\Theta \equiv \{\beta^2, \alpha, \Omega_c, h, \Omega_b, \sigma_8, \log(A)\}$ (right column, h and n_s both fixed to their reference values).

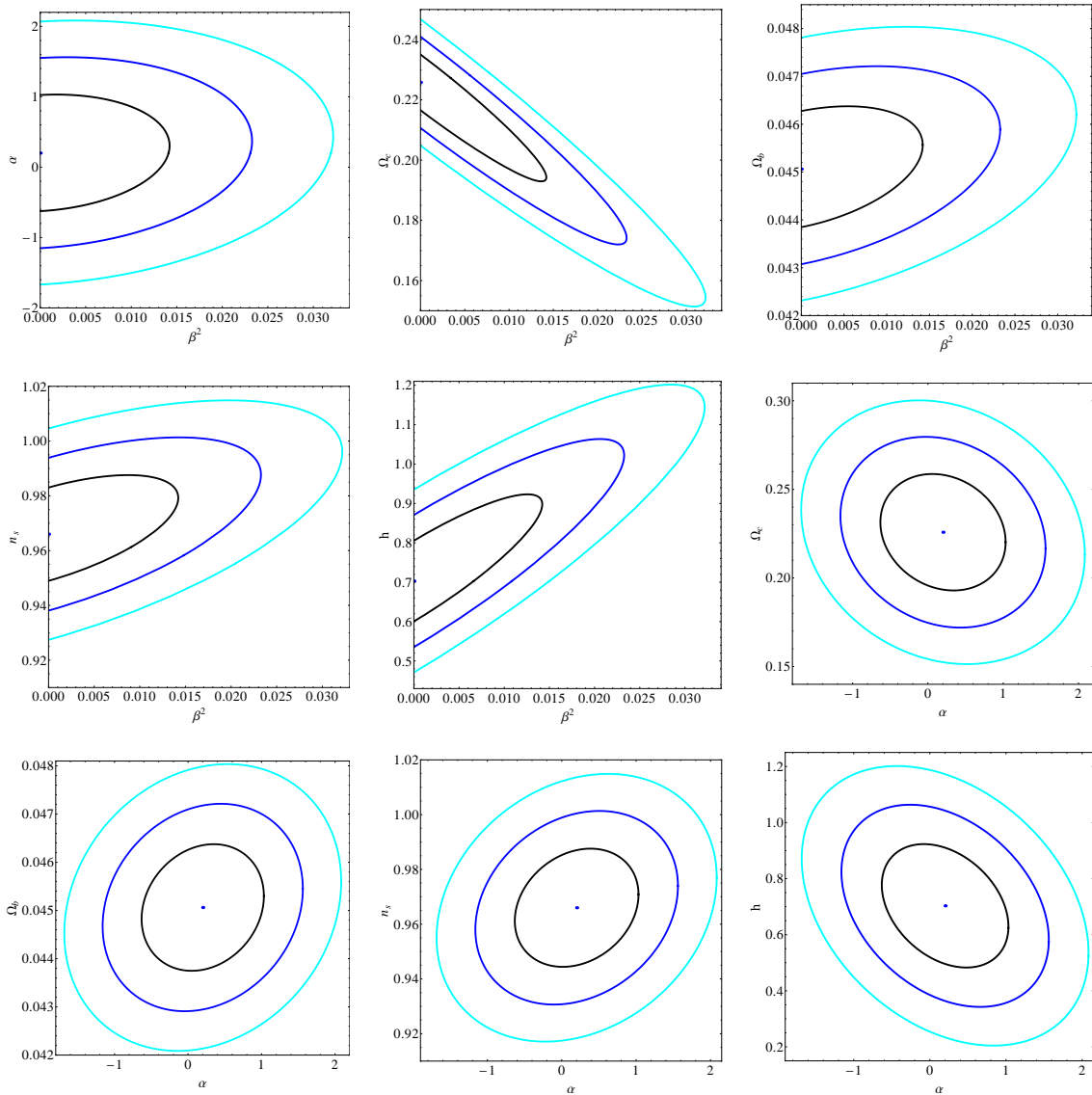


Figure 3: Predicted confidence contours for the cosmological parameter set $\Theta \equiv \{\beta^2, \alpha, \Omega_c, h, \Omega_b, n_s, \log A\}$ using CMB Planck specifications.

V. RESULTS FOR THE GALAXY POWER SPECTRUM

The main effects of the coupling on the matter power spectrum are the shift in the matter-radiation equality, the change in location and amplitude of the BAO and the speed up in the perturbation growth. As already noted, since dark matter dilutes faster for larger $|\beta|$, there is more dark matter in the past than in uncoupled cases and therefore the equality moves to higher redshifts. This implies that the wavelenghts at which perturbations reenter during radiation domination are smaller and thus the power spectrum turnaround moves to smaller scale. Just as for the CMB, the acoustic peaks also move to smaller scales and their amplitude is reduced. These effects are clearly visible in Figs. (6,7). The difference in the parameter growth function is plotted in Fig.(6). In Fig.(7) we make manifest the effect of the coupling on baryonic acoustic oscillations. For each β we plot the ratio between the power spectrum and its smooth spectrum (obtained reducing the amount of baryons in the CAMB code). The ratios are then normalized to high momenta k . As we can see the coupling affects both the amplitude and position of the BAO peaks, shifting them to higher momenta. The effect of β on $P(k, z)$ is therefore quite strong since it occurs simultaneously on the wiggle position and amplitude, on the broad spectrum shape, and on the growth. This results in a tight constraint on the coupling parameter.

Following [50], we build a function that provides the observed linear spectrum at all redshifts and for all cosmological

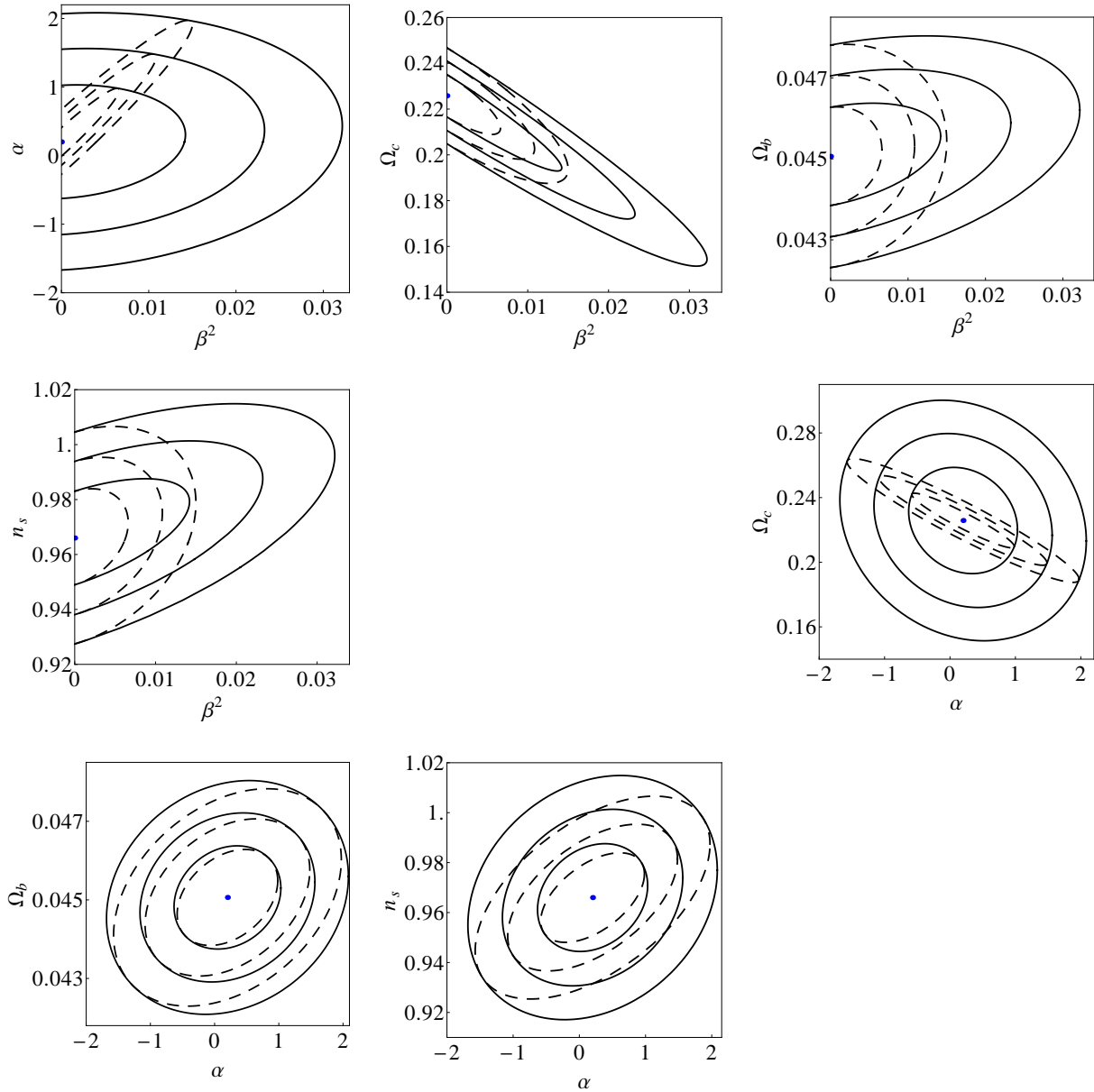


Figure 4: Predicted confidence contours for the cosmological parameter set $\Theta \equiv \{\beta^2, \alpha, \Omega_c, h, \Omega_b, n_s, \log A\}$ (in black, equal to Fig. (3)) using CMB Planck specifications. Overplotted in dashed are the predicted confidence contours for the cosmological parameter set $\{\beta^2, \alpha, \Omega_c, \Omega_b, n_s, \log A\}$, with h fixed to the reference value.

parameters:

$$P_{r,obs}(k_r, \mu_r; z) = P_s(z) + \frac{D_r^2(z)H(z)}{D^2(z)H_r(z)} G^2(z) b^2(z) \sigma_8^2 (1 + \beta_d(z) \mu^2)^2 P(k, z=0), \quad (18)$$

where $G(z)$ is the growth factor, $b(z)$ is the bias, $\beta_d(z)$ is the redshift-distortion factor, $P(k, z=0)$ is the undistorted linear matter spectrum at $z=0$ normalized to unity, μ is the direction cosine, D and H are the angular diameter distance and the Hubble rate at the shell redshift z , respectively, and $P_s(z)$ is the z -dependent shot-noise correction, to be marginalized over in every redshift bin. The subscript r (for ‘reference’) indicates quantities calculated in the fiducial model. In linear theory we have $\beta_d(z) = f(z)/b(z)$ where $f(z) = d \log G / d \log a$ is the growth rate.

In this case, the Fisher matrix for every redshift bin shell is [50],

$$F_{ij} = \frac{1}{8\pi^2} \int_{-1}^{+1} d\mu \int_{k_{min}}^{k_{max}} k^2 dk \frac{\partial \ln P_{obs}(k, \mu)}{\partial \theta_i} \frac{\partial \ln P_{obs}(k, \mu)}{\partial \theta_j} \left[\frac{n(z) P_{obs}(k, \mu)}{n(z) P_{obs}(k, \mu) + 1} \right]^2 V_s. \quad (19)$$

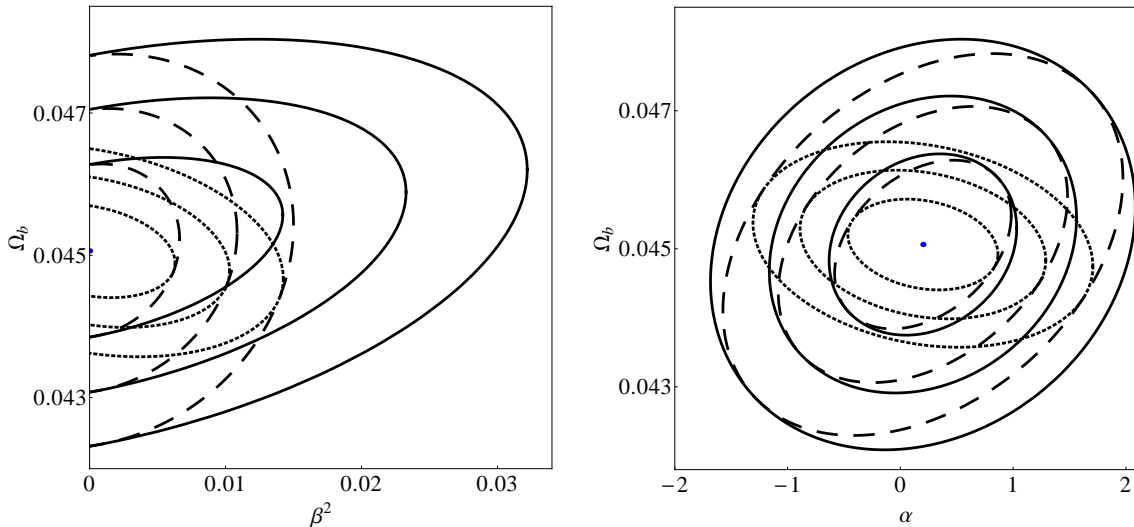


Figure 5: Predicted confidence contours for the cosmological parameter set $\Theta \equiv \{\beta^2, \alpha, \Omega_c, h, \Omega_b, n_s, \log A\}$ (in black, equal to fig.(4)) using CMB Planck specifications. Overplotted are the predicted confidence contours for the cosmological parameter set $\{\beta^2, \alpha, \Omega_c, \Omega_b, n_s, \log A\}$ (dashed contours, with h fixed to the reference values) and the cosmological parameter set $\{\beta^2, \alpha, \Omega_c, \Omega_b, \log A\}$ (dotted contours, with h and n_s fixed to the reference values).

where $n(z)$ is the galaxy number density at redshift z and V_s is the survey volume of the redshift shell. The power spectrum at $z = 0$ and the functions $G(z), H(z), D(z)$ are all obtained numerically by solving the background and perturbation equations of the system for each value of the parameters and the derivatives in F_{ij} are evaluated numerically. We follow [6, 8, 51] and instead of marginalizing over G and f we express them in function of the parameters; in particular we form the combination $g(z) \equiv Gf\sigma_8$ for each redshift bin and write

$$G^2(z)b^2(z)\sigma_8^2(1 + \beta_d(z)\mu^2)^2 P(k, z = 0) = \frac{g(z)^2}{\beta_d(z)^2} (1 + \beta_d(z)\mu^2)^2 P(k, z = 0)$$

and we marginalize over $\beta_d(z)$ assuming an independent parameter β_d for every redshift bin. The prescription for k_{max} is that the variance in cells $\sigma^2(k_{max}, z) = 0.25$, resulting in a $k_{max} = 0.16h/\text{Mpc}$ for the first shell at $z = 0.6$. This conservative cut of the higher momenta allows us to discard the problem of the non-linear correction.

Here and in the next section we have a new parameter, namely σ_8 , whose fiducial is fixed to 0.8. In principle, the parameter $\log A$ employed in the CMB section is related to σ_8 and therefore we should not count them separately. However, the two normalizations are taken at very different epochs and we are being conservative by assuming them to be independent.

We use specifications for a Euclid-like mission based on the Euclid Red Book [3]. The fiducial bias $b(z)$ follows [52]; we adopt redshift bins of $\Delta z = 0.1$ between $0.5 < z < 2$ and a sky coverage of 15,000 sq. deg. [3]. The expected number of $H\alpha$ emitters per deg^2 between $z - dz/2$ and $z + dz/2$ is computed for $H\alpha$ flux $F_{H\alpha} = 4.00 \times 10^{-16} \text{erg/s/cm}^2$ according to [53]. In Fig. (8) we show the expected confidence regions from galaxy power spectra.

The Euclid-like $P(k)$ probe gives in general better constraints than Planck (and also WL, see below), as pointed out in [3]. This applies also to the coupling parameter β : we find indeed $\beta^2 < 0.0015$, a constraint six times stronger than for Planck CMB.

VI. RESULTS FOR WEAK LENSING

An excellent probe for dark energy parameters that complements the aforementioned techniques is weak lensing (see [54] for an extensive treatment), due to the sensitivity with respect to the growth of structure and equal treatment of dark and baryonic matter. The weak lensing power spectrum depending on the multipole ℓ can be written in terms

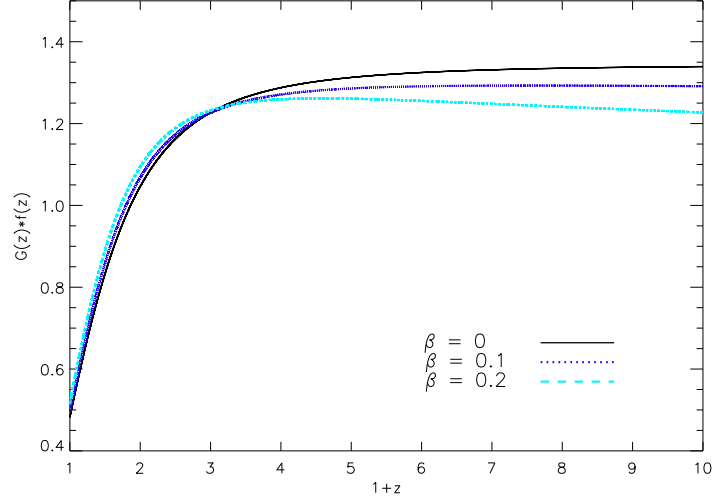


Figure 6: The combination $G(z)f(z)$ that appears as the amplitude of the power spectrum, for various values of β . $G(z)$ is normalized to unity today.

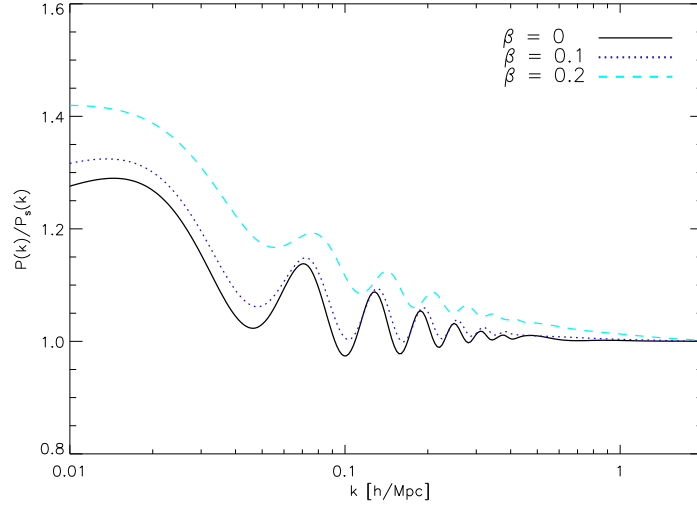


Figure 7: BAO oscillations in $P(k)$ for three values of β . The curves show the ratio $P(k)/P_s(k)$, where $P_s(k)$ is the corresponding smooth power spectrum.

of the matter power spectrum as [55]

$$P(\ell) = \frac{9}{4} \int_0^\infty dz \frac{W^2(z) H^3(z) \Omega_m^2(z)}{(1+z)^4} P_m \left(\frac{\ell}{\pi r(z)} \right), \quad (20)$$

where

$$W(z) = \int_z^\infty d\tilde{z} \left(1 - \frac{r(z)}{r(\tilde{z})} \right) n(\tilde{z}) \quad (21)$$

is the window function and

$$n(z) = z^2 \exp \left(-(z/z_0)^{3/2} \right) \quad (22)$$

the normalized galaxy distribution function [56]. Note that z_0 is related to the median redshift via $z_{\text{med}} \approx 1.412z_0$.

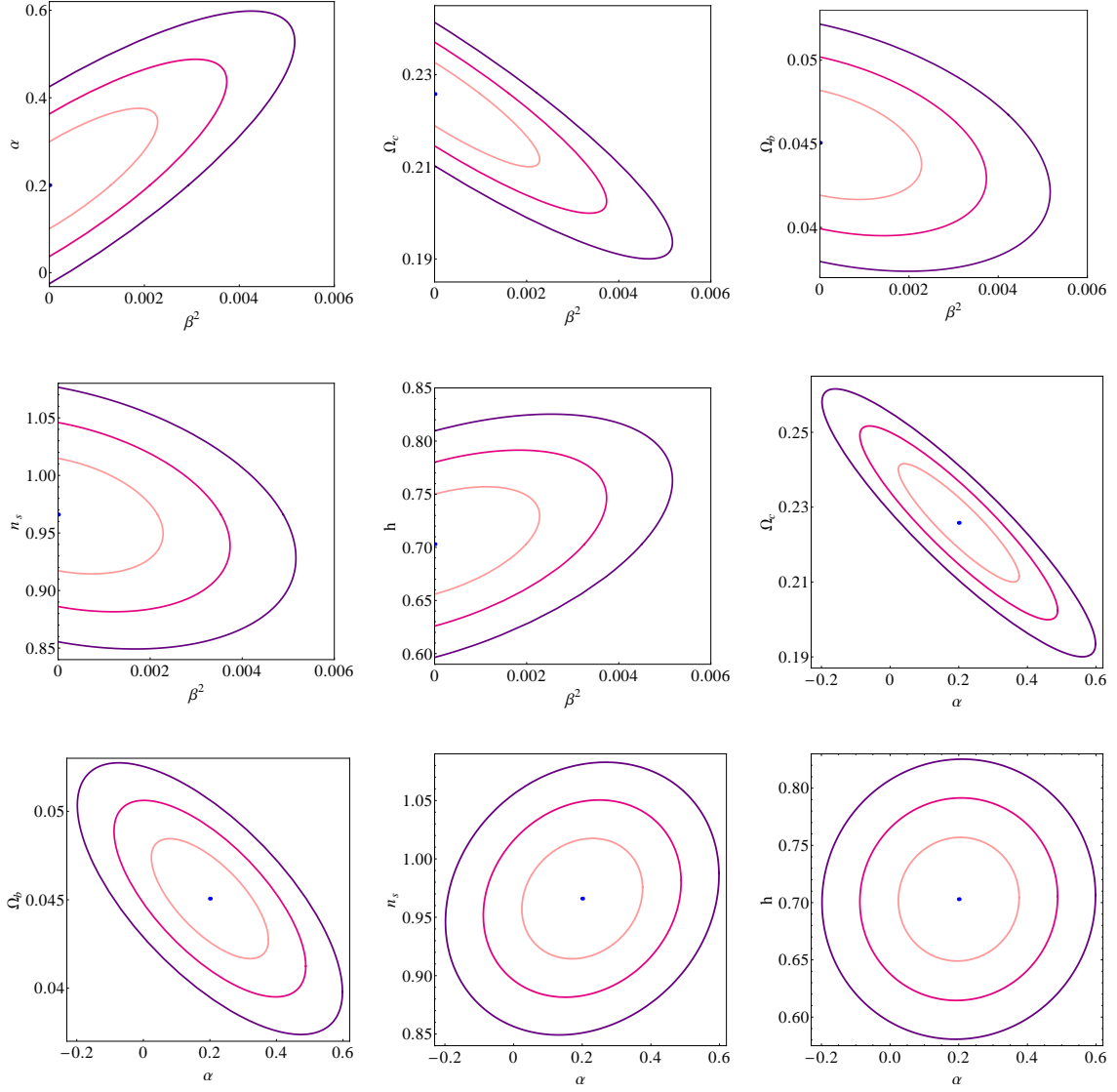


Figure 8: Predicted confidence contours for the cosmological parameter set $\Theta \equiv \{\beta^2, \alpha, \Omega_c, h, \Omega_b, n_s, \sigma_8\}$ using the galaxy power spectrum.

In order to extract as much information from the cosmic shear as possible, we will also employ the so-called weak lensing tomography [57], where we form $\mathcal{N} = 5$ redshift bins and compute the cross-correlation and power spectrum of the shear field. With this, eq. (20) becomes [57]

$$P_{ij}(\ell) = \frac{9}{4} \int_0^\infty dz \frac{W_i(z)W_j(z)H^3(z)\Omega_m^2(z)}{(1+z)^4} P_m\left(\frac{\ell}{\pi r(z)}\right), \quad (23)$$

where $W_i(z)$ now depends on $n_i(z)$, the galaxy distribution in the i -th redshift bin. The binned galaxy distribution is normalized to unity and has been convolved with a Gaussian to account for photometric redshift errors $\Delta_z(1+z)$, i.e.

$$n_i(z) = A_i \int_{i\text{-th bin}} n(\tilde{z}) \exp\left(\frac{-(\tilde{z}-z)^2}{2(\Delta_z(1+\hat{z}_i))^2}\right) d\tilde{z} \quad (24)$$

where \hat{z}_i is the center of the i -th redshift bin and A_i a normalization factor. In Fig. (9) we show the convergence power spectrum for three values of β . The behavior is not trivial since the spectra are a convolution of background and perturbation evolution.

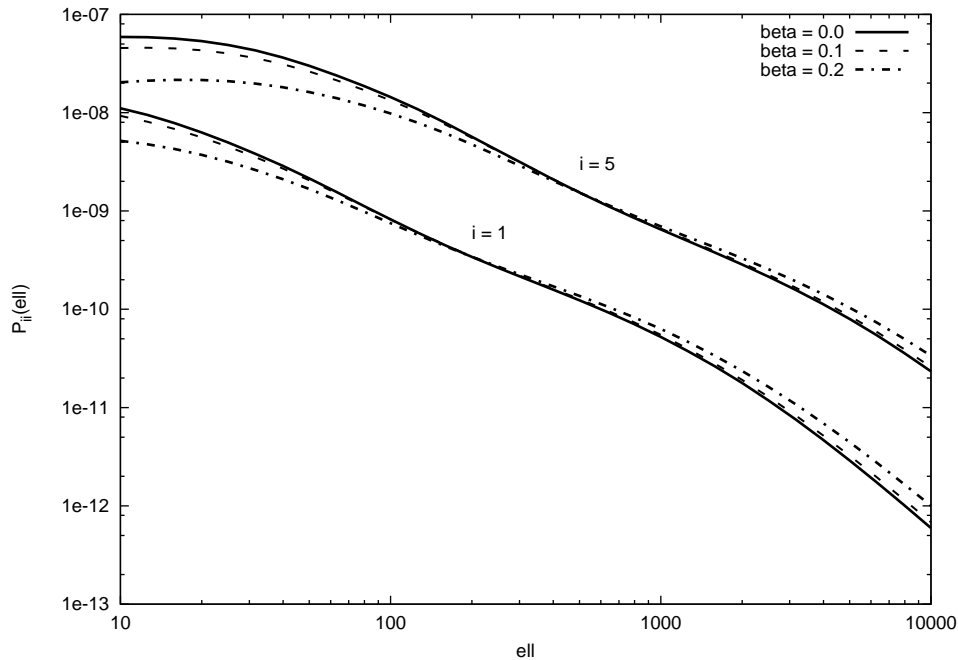


Figure 9: The convergence power spectra P_{11} and P_{55} for three values of β .

The Fisher matrix for the weak lensing power spectrum is then given by [58]

$$F_{\alpha\beta} = f_{\text{sky}} \sum_{\ell, i, j, k, m} \frac{(2\ell + 1)\Delta\ell}{2} \frac{\partial P_{ij}(\ell)}{\partial\theta_\alpha} C_{jk}^{-1} \frac{\partial P_{km}(\ell)}{\partial\theta_\beta} C_{mi}^{-1} \quad (25)$$

with the covariance matrix

$$C_{ij} = P_{ij} + \delta_{ij}\gamma_{\text{int}}^2 n_i^{-1}, \quad (26)$$

where $\gamma_{\text{int}} = 0.22$ in the shot noise term is the intrinsic galaxy ellipticity [56] and

$$n_i = 3600 \left(\frac{180}{\pi}\right)^2 n_\theta / \mathcal{N} \quad (27)$$

with n_θ being the total number of galaxies per arcmin², assuming that the redshift bins have been chosen such that each contain the same amount of galaxies. Since we consider multipoles up to $\ell_{\text{max}} = 5000$, we need to apply non-linear corrections to the matter power spectrum, for which we use the fitting formulae from Ref. [59]. It is clear that this is far from satisfactory since these non-linear corrections are calibrated through Λ CDM N -body simulations and should not be used outside these cases. However at the moment there are no suitable analytical extensions to coupled models (for a recent effort in this direction see e.g. [41]) so we cannot improve on this. Moreover, since our fiducial is indeed almost a Λ CDM cosmology we can assume that the non-linear correction does not introduce a large bias in our results.

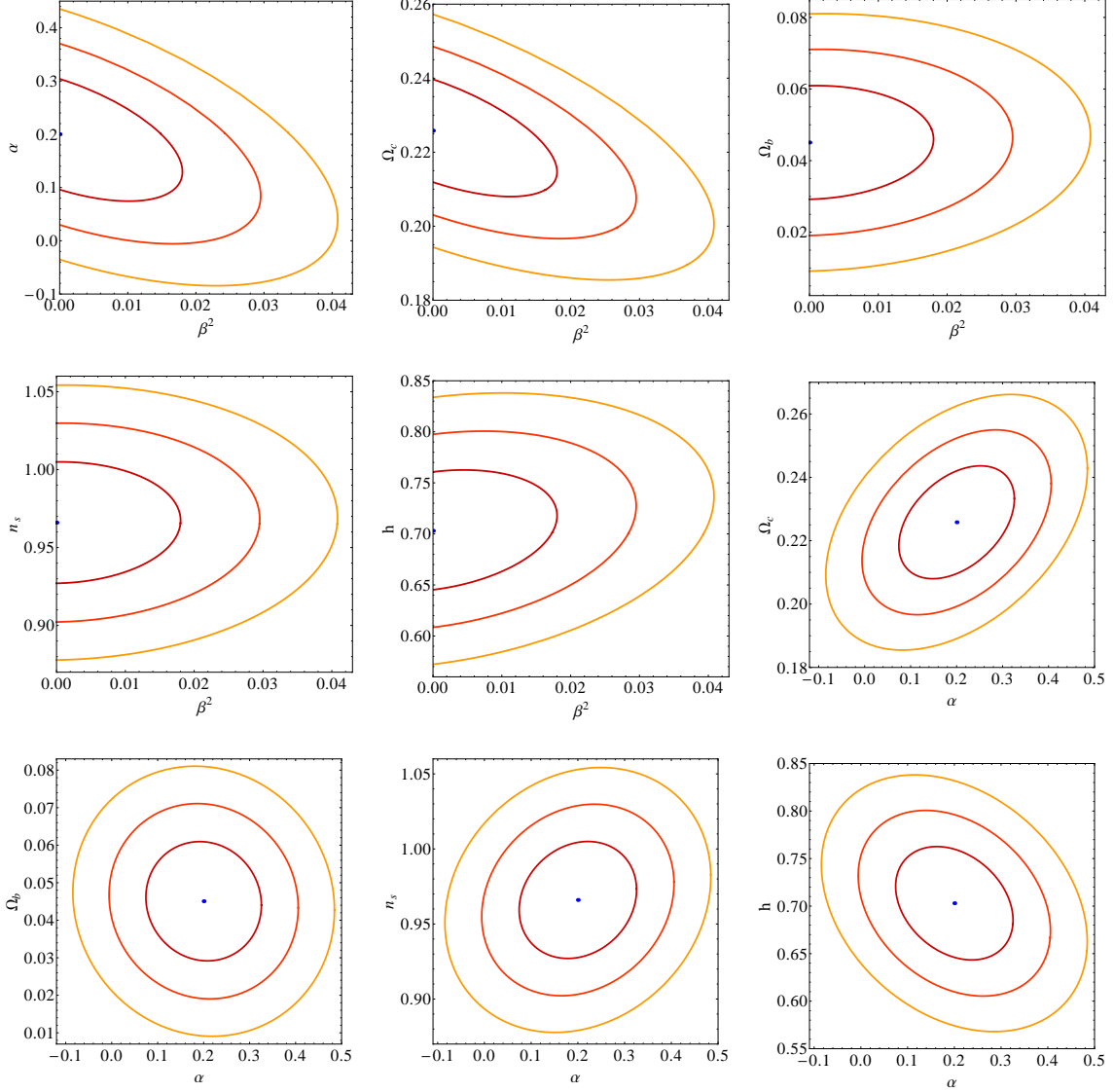
As before, we select a Euclid-like mission as our probe. We use the specifications listed in Table V, as taken from the Euclid Red Book [3]. In Fig. (10) we show the marginalized confidence contours. The WL constraint on β^2 is 0.012, weaker than either CMB or $P(k)$. Interestingly, however, the constraint on the potential slope α is the strongest among the various probes.

VII. COMBINING CMB, P(K) AND WL

In this Section we finally combine all the results of the various probes. The combination of $P(k)$ and WL is not totally accurate since the two probes are assumed to be independent while in fact they observe the same field of galaxies and the lensing signal is correlated with the density distribution. However, since as we have seen the

Parameter	Value	Description
A	15 000 deg ²	Survey area
n_θ	30	Galaxies per arcmin ²
ℓ_{\max}	5000	Maximum multipole
z_{med}	0.9	Median redshift
Δ_z	0.05	Photometric redshift error

Table V: Mission goals for a Euclid-like project. [3]

Figure 10: Predicted confidence contours for the cosmological parameter set $\Theta \equiv \{\beta^2, \alpha, \Omega_c, h, \Omega_b, n_s, \sigma_8\}$ using weak lensing Euclid-like specifications.

constraints from $P(k)$ are in general quite stronger, we expect that an improved treatment will not change drastically our results.

The combined Fisher confidence regions are plotted in Fig.(11) and (12) and the results are in Table (VII). The main result is that future surveys can constrain the coupling of dark energy to dark matter β^2 to less than $3 \cdot 10^{-4}$.

We can ask whether a better knowledge of the parameters $\{\alpha, \Omega_c, h, \Omega_b, n_s, \sigma_8, \log(A)\}$, obtained by independent future observations, can give us better constraints on the coupling β^2 . In Table VII we list the $1\text{-}\sigma$ error on β^2 obtained

Parameter	σ_i CMB+ $P(k)$	σ_i CMB+ $P(k)$ +WL
β^2	0.00051	0.00032
α	0.055	0.032
Ω_c	0.0037	0.0010
h	0.0080	0.0048
Ω_b	0.00047	0.00041
n_s	0.0057	0.0049
σ_8	0.0049	0.0036
$\log(A)$	0.0051	0.0027

Table VI: $1-\sigma$ errors for the set $\Theta \equiv \{\beta^2, \alpha, \Omega_c, h, \Omega_b, n_s, \sigma_8, \log(A)\}$ of cosmological parameters, combining CMB+ $P(k)$ (left column) and CMB+ $P(k)$ +WL (right column).

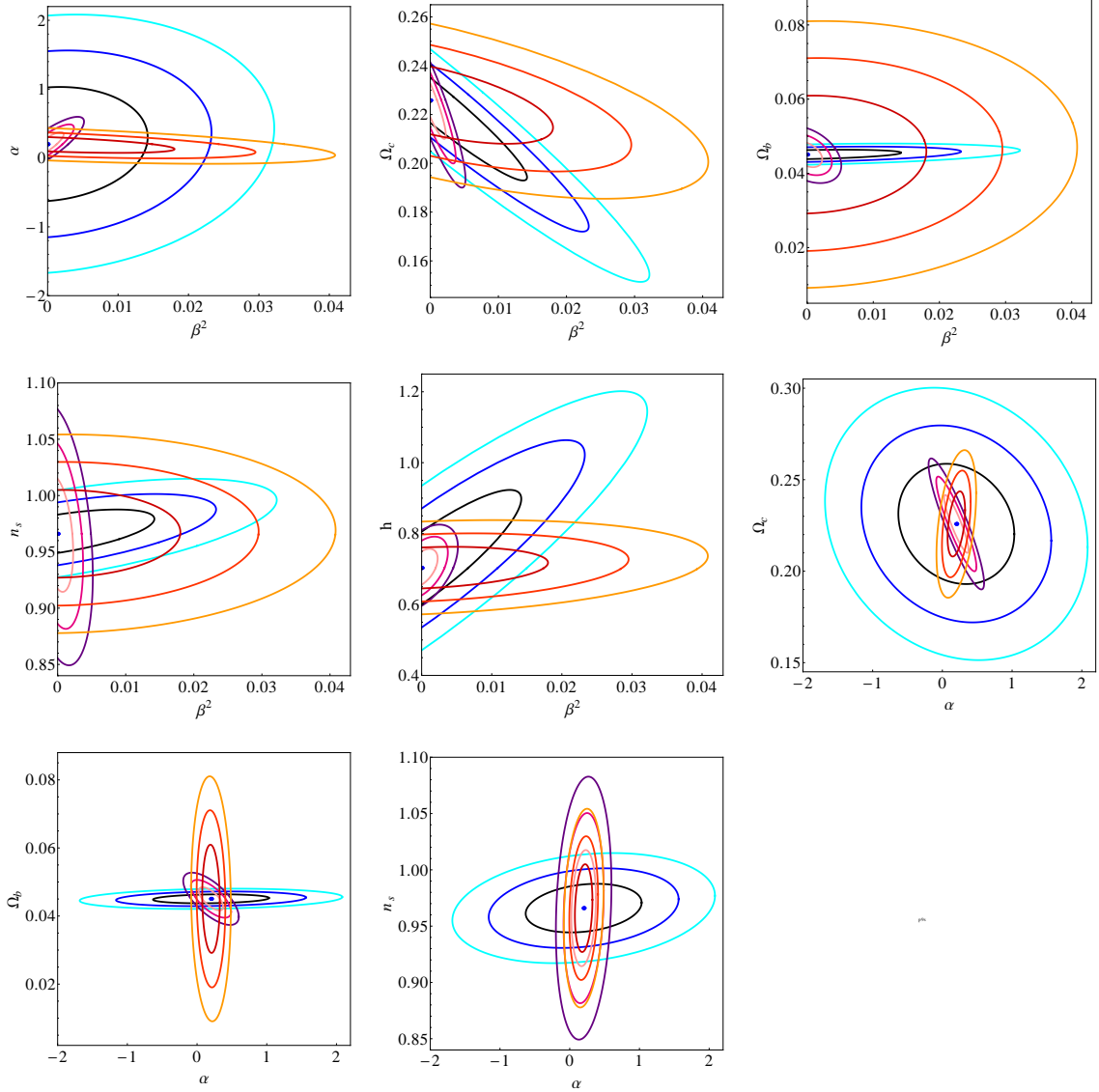


Figure 11: Comparison among predicted confidence contours for the cosmological parameter set $\Theta \equiv \{\beta^2, \alpha, \Omega_c, h, \Omega_b, n_s, \sigma_8, \log(A)\}$ using CMB (Planck, blue contours), $P(k)$ (pink-violet contours) and weak lensing (orange-red contours) with Euclid-like specifications.

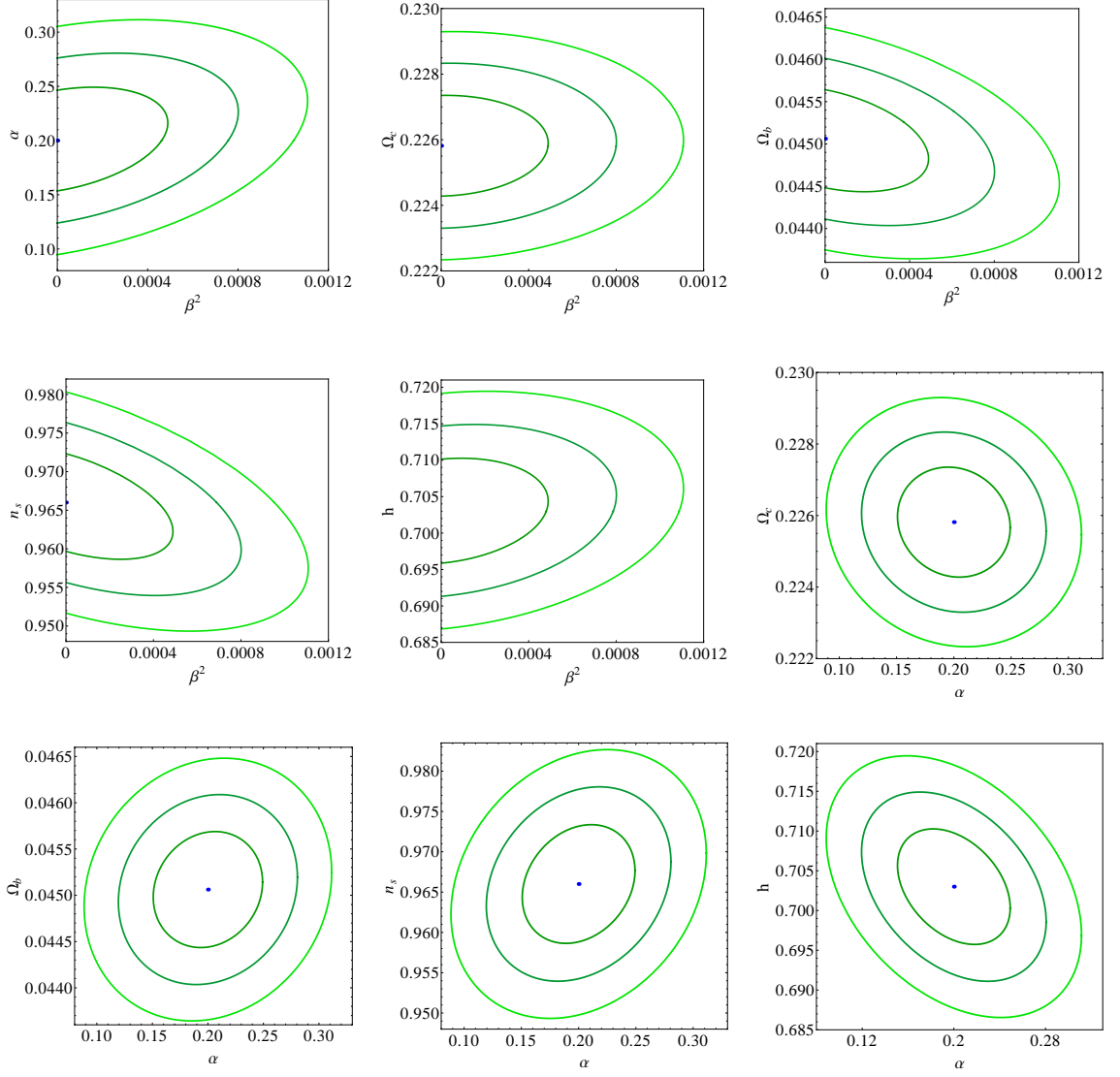


Figure 12: Combined predicted confidence contours for the cosmological parameter set $\Theta \equiv \{\beta^2, \alpha, \Omega_c, h, \Omega_b, n_s, \sigma_8, \log(A)\}$ from CMB (Planck), $P(k)$ and weak lensing (Euclid-like) specifications.

when we fix, one after the other, each of the remaining parameters to their reference value instead of marginalizing. P_1 corresponds to fixing one parameter (α) and marginalize over all the others, P_2 corresponds to fixing two parameters (α and Ω_c) and marginalize over all the others and so on until P_7 where we estimate the error on β^2 when we fix all parameters.

The first column corresponds to the effect on CMB only. CMB alone gains the most from a better knowledge of the parameters. In this case the error on β^2 improves by almost one order of magnitude when Ω_c is fixed (thanks to the degeneracy with this parameter) and of almost two orders of magnitude when also h and Ω_b are known. A better knowledge of $\alpha, \Omega_c, h, \Omega_b$ makes CMB constraints alone comparable to the combination of all probes (when all parameters are marginalized over).

$P(k)$ observations (second column) improve bounds by almost an order of magnitude when $\alpha, \Omega_c, h, \Omega_b$ have been fixed, becoming even better than the ones obtained in the marginalized combination of all probes. The third column shows weak lensing constraints, which gain one order of magnitude when all parameters are known: note that in this case the amplitude of perturbations σ_8 is still relevant even when all previous parameters have already been fixed.

The last column combines all three probes. Interestingly, the combination of CMB, power spectrum and weak lensing is already very good when all parameters are marginalized over; no much gain is obtained, overall, by a better knowledge of the other parameters. This is confirmed also when looking at Table VIII. Here we show the errors on

Set of fixed parameters	CMB	$P(k)$	WL	CMB + $P(k)$ + WL
(Marginalized on all params)	0.0094	0.0015	0.012	0.00032
$P_1 = \{\alpha\}$	0.0093	0.00085	0.0098	0.00030
$P_2 = \{P_1\} \cup \{\Omega_c\}$	0.0026	0.00065	0.0084	0.00030
$P_3 = \{P_2\} \cup \{h\}$	0.00054	0.00040	0.0076	0.00026
$P_4 = \{P_3\} \cup \{\Omega_b\}$	0.00033	0.00028	0.0037	0.00020
$P_5 = \{P_4\} \cup \{n_s\}$	0.00033	0.00024	0.0034	0.00019
$P_6 = \{P_5\} \cup \{\sigma_8\}$	0.00033	0.00024	0.0017	0.00019
$P_7 = \{P_6\} \cup \{\log(A)\}$	0.00032	0.00024	0.0017	0.00019

Table VII: $1-\sigma$ errors for β^2 , for CMB, $P(k)$, WL and CMB+ $P(k)$ +WL. For each line the set of parameters P_i has been fixed to the reference value. The first line corresponds to the case in which we have marginalized over all parameters.

Fixed parameter	CMB	$P(k)$	WL	CMB + $P(k)$ + WL
(Marginalized on all params)	0.0094	0.0015	0.012	0.00032
α	0.0093	0.00085	0.0098	0.00030
Ω_c	0.0026	0.00066	0.0093	0.00032
h	0.0044	0.0013	0.011	0.00032
Ω_b	0.0087	0.0014	0.012	0.00030
n_s	0.0074	0.0014	0.012	0.00028
σ_8	0.0094	0.00084	0.0053	0.00030
$\log(A)$	0.0090	0.0015	0.012	0.00032

Table VIII: $1-\sigma$ errors for β^2 , for CMB, $P(k)$, WL and CMB+ $P(k)$ +WL. For each line, only the parameter in the left column has been fixed to the reference value. The first line corresponds to the case in which we have marginalized over all parameters.

β^2 when we have a better knowledge of only one other parameter, which is here fixed to the reference value. All remaining parameters are marginalized over. The combination of CMB, power spectrum and weak lensing is already a powerful tool and a better knowledge of one parameter doesn't improve much the constraints on β^2 . CMB alone, instead, improves by a factor 3 when Ω_c is known and by a factor 2 when h is known. The power spectrum is mostly influenced by Ω_c , which allows to improve constraints on the coupling by more than a factor 2. Weak lensing gains the most by a better knowledge of σ_8 .

The constraint on β^2 can be easily converted into a constraint on the Brans-Dicke coupling parameter ω_{BD} since (see e.g. [14])

$$3 + 2\omega_{BD} = \frac{1}{2\beta^2} \quad (28)$$

We obtain then

$$\omega_{BD} > 800 \quad (29)$$

The post-Newtonian parameter γ_{PPN} is related (in the limit $\gamma \ll 1$) to ω_{BD} as $\gamma_{PPN} = 1 - 2/(2\omega_{BD} + 3)$ so that our final predicted constraint on β^2 reflects into a constraint

$$|\gamma_{PPN} - 1| < 1.2 \times 10^{-3} \quad (30)$$

This is still two orders of magnitude weaker than the limits on a scalar coupling to baryons obtained in laboratory or solar system experiments, of the order of $|\gamma_{PPN} - 1| < 10^{-5}$ (see e.g. [24, 25, 60]) but of course the cosmological bounds are complementary to the local measurements since here we deal with the coupling to dark matter.

VIII. CONCLUSIONS

Future cosmological surveys will measure the properties of our universe to a unprecedented precision. This will allow not only to measure the main cosmological parameters but also to test models that challenge the standard

scenario of particle physics and cosmology. The two main tools of observational cosmology, namely cosmic microwave background and large-scale structure, can be combined to extract the maximal amount of information.

In this paper we combined forecasts from the Planck CMB experiment and from future redshift surveys and weak lensing surveys based on the proposed Euclid satellite to get constraint on a model of coupled dark energy. In this model, dark energy mediates a force acting on dark matter and produces an additional attractive interaction which modifies Einstein's gravity. The coupling parameter β^2 measures the amount of this modification. We find that combining Planck with a Euclid-like survey can constrain β^2 to a level of $3 \cdot 10^{-4}$, two orders of magnitude better than current constraints [20, 22]; this bound is weaker but complementary to the small-scale limits set by local gravity tests on Yukawa corrections (see e.g. [24, 25]). A better knowledge of Ω_c , h , n_s can improve the precision of measurement of the coupling as obtained by CMB measurements, due to manifest degeneracies among these parameters and the fifth force as measured by β^2 . Interestingly though, the combination of CMB, power spectrum and weak lensing is already so powerful that no much gain is obtained, overall, by a better knowledge of the other parameters. In this sense, these three probes are optimally complementary probes of the dark energy-dark matter coupling.

Acknowledgments

Support was given to V.P. and C.Q. by the Italian Space Agency through the ASI contracts Euclid-IC (I/031/10/0). V.P. is also supported by the Young Scientist SISSA Grant. Support was given to L.A. by the Deutsche Forschungsgemeinschaft through the programme TRR33 "The Dark Universe". We acknowledge the Euclid Consortium for the preparation of the Euclid Red Book, the Euclid Science Coordinators for reviewing the draft of this paper and the Euclid Theory Working Group for very fruitful exchange of ideas. We thank C. Carbone and C. Baccigalupi for useful comments and discussion.

-
- [1] J. K. e. Adelman-McCarthy, *Astrophys. J. Supp.* **175**, 297 (2008), [arXiv:0707.3413](#).
 - [2] M. Colless, G. Dalton, S. Maddox, W. Sutherland, P. Norberg, S. Cole, J. Bland-Hawthorn, T. Bridges, R. Cannon, C. Collins, et al., *VizieR Online Data Catalog* **7250** (2007).
 - [3] Euclid Consortium, <http://sci.esa.int/science-e/www/object/index.cfm?fobjectid=48983#> (2011).
 - [4] Z. Ivezić, J. A. Tyson, E. Acosta, R. Allsman, S. F. Anderson, J. Andrew, R. Angel, T. Axelrod, J. D. Barr, A. C. Becker, et al., *ArXiv e-prints* (2008), [arXiv:0805.2366](#).
 - [5] J. J. Mohr, D. Adams, W. Barkhouse, C. Beldica, E. Bertin, Y. D. Cai, L. A. N. da Costa, J. A. Darnell, G. E. Daues, M. Jarvis, et al., in *Society of Photo-Optical Instrumentation Engineers (SPIE) Conference Series* (2008), vol. 7016 of *Society of Photo-Optical Instrumentation Engineers (SPIE) Conference Series*, [arXiv:0807.2515](#).
 - [6] Y. Wang, W. Percival, A. Cimatti, P. Mukherjee, L. Guzzo, C. M. Baugh, C. Carbone, P. Franzetti, B. Garilli, J. E. Geach, et al., *Monthly Notices of the Royal Astronomical Society* (2010), [arXiv:1006.3517v2\[astro-ph.CO\]](#).
 - [7] M. Martinelli, L. L. Honorez, A. Melchiorri, and O. Mena, *Phys. Rev. D* **81**, 103534 (2010), [arXiv:1004.2410](#).
 - [8] C. Di Porto, L. Amendola, and E. Branchini, *ArXiv e-prints* (2011), [arXiv:1101.2453](#).
 - [9] F. De Bernardis, M. Martinelli, A. Melchiorri, O. Mena, and A. Cooray (2011), [arXiv:1104.0652](#).
 - [10] C. Carbone, L. Verde, Y. Wang, and A. Cimatti, *J. Cosm. Astroparticle Phys.* **3**, 30 (2011), [arXiv:1012.2868](#).
 - [11] L. Amendola and S. Tsujikawa, *Dark Energy: Theory and Observations* (Cambridge University Press, 2010), ISBN 0521516005.
 - [12] C. Wetterich, *Astron. Astrophys.* **301**, 321 (1995), [arXiv:hep-th/9408025](#).
 - [13] L. Amendola, *Physical Review D* **62**, 43511 (1999), [arXiv:9908023](#).
 - [14] V. Pettorino and C. Baccigalupi, *Phys. Rev. D* **77**, 103003 (2008), [arXiv:0802.1086](#).
 - [15] P. Peebles and B. Ratra, *Reviews of Modern Physics* **75**, 559 (2003), [arXiv:0207347v2](#).
 - [16] R. Mainini and S. Bonometto, *J. Cosm. Astroparticle Phys.* **9**, 17 (2007), [arXiv:0709.0174](#).
 - [17] M. Baldi, *MNRAS* **411**, 1077 (2011), [arXiv:1005.2188](#).
 - [18] J. Beyer, S. Nurmi, and C. Wetterich, *Phys. Rev. D* **84**, 023010 (2011), [arXiv:1012.1175](#).
 - [19] L. Amendola, C. Quercellini, D. Tocchini-Valentini, and A. Pasqui, *Astrophys. J. Lett.* **583**, L53 (2003), [arXiv:astro-ph/0205097](#).
 - [20] L. Amendola and C. Quercellini, *Phys. Rev. D* **68**, 023514 (2003), [arXiv:astro-ph/0303228](#).
 - [21] R. Bean, E. E. Flanagan, I. Laszlo, and M. Trodden, *Phys. Rev. D* **78**, 123514 (2008), [arXiv:0808.1105](#).
 - [22] G. La Vacca, J. R. Kristiansen, L. P. L. Colombo, R. Mainini, and S. A. Bonometto, *JCAP* **0904**, 007 (2009), [arXiv:0902.2711](#).
 - [23] J.-P. Uzan, *Reviews of Modern Physics* **75**, 403 (2003), [arXiv:hep-ph/0205340](#).
 - [24] D. J. Kapner, T. S. Cook, E. G. Adelberger, J. H. Gundlach, B. R. Heckel, C. D. Hoyle, and H. E. Swanson, *Physical Review Letters* **98**, 021101 (2007), [arXiv:hep-ph/0611184](#).
 - [25] K. Nakamura et al. (Particle Data Group), *J. Phys.* **G37**, 075021 (2010).

- [26] J. Khoury and A. Weltman, *Physical Review Letters* **93**, 171104 (2004), [arXiv:astro-ph/0309300](#).
- [27] L. Hui, A. Nicolis, and C. Stubbs, *Phys.Rev.* **D80**, 104002 (2009), [arXiv:0905.2966](#).
- [28] G. Dvali, *New Journal of Physics* **8**, 326 (2006), [arXiv:hep-th/0610013](#).
- [29] E. J. Copeland, A. R. Liddle, and D. Wands, *Phys. Rev.* **D57**, 4686 (1998), [arXiv:gr-qc/9711068](#).
- [30] G. Mangano, G. Miele, and V. Pettorino, *Mod. Phys. Lett.* **A18**, 831 (2003), [arXiv:astro-ph/0212518](#).
- [31] L. Amendola, *Physical Review D* **69**, 103524 (2004), [arXiv:0311175v2](#).
- [32] T. Koivisto, *Phys. Rev.* **D72**, 043516 (2005), [arXiv:astro-ph/0504571](#).
- [33] Z.-K. Guo, N. Ohta, and S. Tsujikawa, *Phys. Rev.* **D76**, 023508 (2007), [arXiv:astro-ph/0702015](#).
- [34] C. Quercellini, M. Bruni, A. Balbi, and D. Pietrobon, *Phys. Rev. D* **78**, 063527 (2008), [arXiv:0803.1976](#).
- [35] M. Quartin, M. O. Calvao, S. E. Joras, R. R. R. Reis, and I. Waga, *JCAP* **0805**, 007 (2008), [arXiv:0802.0546](#).
- [36] J. Valiviita, R. Maartens, and E. Majerotto, *Mon.Not.Roy.Astron.Soc.* **402**, 2355 (2010), [arXiv:0907.4987](#).
- [37] N. Wintergerst and V. Pettorino, *Phys.Rev.* **D82**, 103516 (2010), [arXiv:1005.1278](#).
- [38] R. Mainini and S. Bonometto, *Phys.Rev.* **D74**, 043504 (2006), [arXiv:astro-ph/0605621](#).
- [39] F. Saracco, M. Pietroni, N. Tetradis, V. Pettorino, and G. Robbers, *Phys.Rev.* **D82**, 023528 (2010), [arXiv:0911.5396](#).
- [40] M. Baldi and V. Pettorino, *Mon.Not.Roy.Astron.Soc.* **412**, L1 (2011), [arXiv:1006.3761](#).
- [41] M. Baldi, V. Pettorino, G. Robbers, and V. Springel, *Mon. Not. Roy. Astron. Soc.* **403**, 1684 (2010).
- [42] J. R. Kristiansen, G. La Vacca, L. P. L. Colombo, R. Mainini, and S. A. Bonometto, *New Astron.* **15**, 609 (2010), [arXiv:0902.2737](#).
- [43] R. Mainini and D. F. Mota (2010), [arXiv:1011.0083](#).
- [44] J.-Q. Xia, *Phys.Rev.* **D80**, 103514 (2009), [arXiv:0911.4820](#).
- [45] R. Laureijs et al. (2009), [arXiv:0912.0914](#).
- [46] D. Larson, J. Dunkley, G. Hinshaw, E. Komatsu, M. Nolta, et al., *Astrophys.J.Suppl.* **192**, 16 (2011), [arXiv:1001.4635](#).
- [47] WMAP 7 year data, http://lambda.gsfc.nasa.gov/product/map/dr4/params/lcdm_sz_lens_wmap7.cfm (2010).
- [48] The Planck Collaboration, *ArXiv Astrophysics e-prints* (2006), [arXiv:astro-ph/0604069](#).
- [49] A. Lewis, A. Challinor, and A. Lasenby, *Astrophys.J.* **538**, 473 (2000), [arXiv:astro-ph/9911177](#).
- [50] H.-J. Seo and D. J. Eisenstein, *Astrophys. J.* **598**, 720 (2003), [arXiv:astro-ph/0307460](#).
- [51] L. Amendola, C. Quercellini, and E. Giallongo, *Monthly Notices of the Royal Astronomical Society* **357**, 429 (2005), [arXiv:0404599](#).
- [52] A. Orsi et al. (2009), [arXiv:0911.0669](#).
- [53] J. E. Geach, A. Cimatti, W. Percival, Y. Wang, L. Guzzo, G. Zamorani, P. Rosati, L. Pozzetti, A. Orsi, C. M. Baugh, et al., *MNRAS* **402**, 1330 (2010), [arXiv:0911.0686](#).
- [54] M. Bartelmann and P. Schneider, *Phys. Rept.* **340**, 291 (2001), [arXiv:astro-ph/9912508](#).
- [55] N. Kaiser, *The Astrophysical Journal* **388**, 272 (1992).
- [56] A. Amara and A. Réfrégier, *Monthly Notices of the Royal Astronomical Society* **381**, 1018 (2007), [arXiv:0610127v2](#).
- [57] W. Hu, *The Astrophysical Journal* **522**, L21 (1999), [arXiv:9904153](#).
- [58] W. Hu and M. Tegmark, *The Astrophysical Journal* **514**, L65 (1999), [arXiv:9811168](#).
- [59] R. E. Smith, J. A. Peacock, A. Jenkins, S. D. M. White, C. S. Frenk, F. R. Pearce, P. A. Thomas, G. Efstathiou, and H. M. P. Couchman, *Monthly Notices of the Royal Astronomical Society* **341**, 1311 (2003), [arXiv:0207664v2](#).
- [60] B. Bertotti, L. Iess, and P. Tortora, *Nature (London)* **425**, 374 (2003).